of the cell interior to be enlarged to fill the entire monitor screen.

The electronic signal generated by the CCTV camera is generally fed to the video tape recorder, and from it another signal is passed on to the CCTV monitor. This provides a check on what is actually being recorded.

TESTING THE SYSTEM

A phase equilibria cell with a 1×4 cm rectanglar window was used. Before assembly, the rear of the cell interior was coated with a mixture of the fluorescent pigment and polystyrene Q-Dope, a low loss coil coating manufactured by GC Electronics. When dried, this even coating resisted any effects of temperature cycling from 77 K to ambient temperature.

The assembled cell was placed in a gas bath cryostat,[2] cooled to 100 K, and pressurized to 25 $MN \cdot m^{-2}$ with a helium–nitrogen mixture. With all components (except the front surfaced aluminum mirror and the flint glass) functioning, the level of the liquid mixture in the cell was raised and lowered by admitting more gas and draining the liquid, respectively. The meniscus appeared as a distinct group of black and white bands on the monitor. The contrast at the interface was excellent. Any changes in the meniscus were easily followed.

Several combinations of lens extensions were tried with the resulting changes in image magnification. The best results were achieved with an extension of 40 mm which yielded an image magnification of approximately 21×. The illumination of the cell interior was sufficiently intense to permit closing the lens aperture several stops.

No difficulties are expected to result from increasing the pressure to 70 $MN \cdot m^{-2}$ and lowering the temperature to 20 K. The effect of pressure on the luminescent efficiency should be negligible[3]. The reduced temperature might narrow the emission peak and increase the output, approaching a maximum near absolute zero.[4]

[1] Mention of specific products is for identification only and does not imply endorsement by the Bureau of Mines.
[2] W. E. DeVaney, L. Rhodes, and P. C. Tully, Cryog. Technol. 7, No. 1 (1971).
[3] H. W. Leverenz, *An Introduction to Luminescence of Solids* (Dover, New York, 1968), p. 152.
[4] Ref. 3, pp. 136–46.

THE REVIEW OF SCIENTIFIC INSTRUMENTS VOLUME 41, NUMBER 10 OCTOBER 1970

A Parallel Plate Electrostatic Spectrograph

T. S. GREEN AND G. A. PROCA
European Space Research Institute, Frascati, Italy
(Received 10 February 1970; and in final form, 8 June 1970)

A description is given of a new parallel plate electrostatic spectrograph. A parallel plate electrostatic analyzer has been discussed previously, in which particles issuing from a point source on the earthed plate are deflected by the electric field and brought to a focus on that plate, provided the angle of entrance to the field is 45°. This is a simple example of the more general focusing properties of a parallel plate analyzer. From consideration of these properties, it has been found possible to select a given angle of entry into the field for which second order focusing can be attained giving rise to an angular aberration term proportional to $(\Delta\theta)^3$. Uslng an acceptance of ±6° a resolving power of 200 is predicted and has been obtained with a prototype.

INTRODUCTION

ANALYSIS of the energies of charged particles can be carried out magnetically or electrostatically. For low energy electrons the magnetic rigidity is so low as to make the magnetic system difficult to use. Instead, one must consider the use of electrostatic systems which in general possess poorer focusing properties than their magnetic counterparts. Beside simple gated systems[1] most analyzers built have been of the 127° focusing type[2] or the 180° type.[3]

A simple parallel plate analyzer was devised by Harrower[4] and Yarnold and Bolton[5] in which electrons are bent in a uniform electric field. For particles emitted at the earth plate (see Fig. 1) at an angle of 45° to the plate there is first order focusing on the plate at a distance away which is proportional to the energy divided by the electric field.

We wish to point out this is a singular, though simple, possibility for using the deflection properties of a parallel plate analyzer. If the source is mounted in the region at

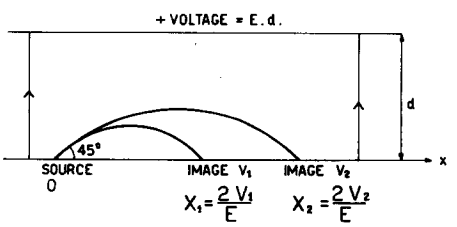

FIG. 1. Schematic of ray paths in parallel plate electrostatic analyzer with mean ray angle of 45° (after Harrower[3] and Yarnold and Bolton[4]).

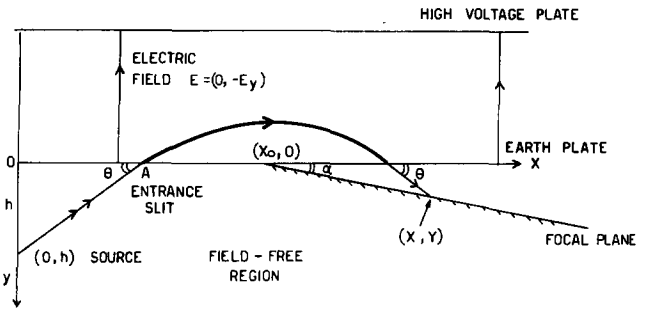

FIG. 2. Ray paths in parallel plate electrostatic analyzer for generalized treatment. Source mounted at $(0,h)$ in the field-free space, mean ray at an angle $-\theta$ to x axis.

earth potential external to the analyzer, and any angle θ is chosen as the mean angle of electrons to the earth plate, then focusing occurs along a line, also in the earth region, whose position depends on the source position and θ. It is found that the angular aberration and the magnification depend on the value of θ. In fact, for $\theta=30°$, the angular aberrations are minimized allowing one to build an analyzer of reasonable resolution with a wide angular acceptance.

I. THEORY OF THE INSTRUMENT

The physical arrangement is shown in Fig. 2. The analyzer consists of two parallel plates separated by a distance d, with a retarding voltage between them. In the analysis we take the earth plate to be the plane $y=0$, the repelling plate being then at $y=-d$; the source is mounted at $x=0$, $y=+h$. The mean ray direction is taken to be at angle $-\theta$ to the x axis.

A. Motion of Electrons

The electron travels in a straight line from the source S to the slit A; on entering the field at an angle θ it is deflected and with a retarding potential one finds that it returns to the earth plate at an x displacement of $(2V/E)\sin2\theta$, where V is the energy in electron volts and E the electric field in volts per centimeter. After exit it again travels in a straight line (Fig. 2). The equation of the electron path in the field free region is then

$$x=(h+y)\cot\theta+(2V/E)(\sin2\theta) \tag{1}$$

(see Appendix I).

B. Focusing Condition

Rays from the same source point $(0, +h)$ with different angles of incidence are brought to a first order focus when $dx/d\theta=0$ for y constant.

Using Eq. (1) one finds $dx/d\theta$ is zero when

$$(h+y)=(4V/E)\cos2\theta\cdot\sin^2\theta. \tag{2}$$

The foci for various values of initial energy V therefore lie on a straight line

$$x=(h+y)\cot\theta\cdot[1+(1/\cos2\theta)]. \tag{3}$$

This line makes an angle α to the x axis where

$$\tan\alpha=\tan\theta\cos2\theta/(1+\cos2\theta).$$

Hence one sees that the condition of a focal line along the earth plane for $\theta=45°$ is only one of an infinite set of possibilities. It is in fact the limiting case. For $\theta>45°$ the focal line is apparently in the space between the plates.

C. Angular Aberrations

The aberrations arise from the fact that while $dx/d\theta$ may be zero, other terms $d^2x/d\theta^2$, etc. are not. The aberrations, arising when using an extreme ray of angle $\theta+\Delta\theta$, may be calculated from the separation of the intercepts with the focal line of the mean ray and the extreme ray. The two rays are

$$x=(h+y)\cot\theta+(2V/E)\sin2\theta \qquad \text{(ray 1)}$$

$$x=(h+y)\cot(\theta+\Delta\theta)+(2V/E)\sin2(\theta+\Delta\theta) \qquad \text{(ray 2)}$$

and the focal line is given by Eq. (3).

If x_1 and x_2 are the abscissas of the two intercepts then $(x_2-x_1)/x_1$ is a measure of the aberration and is given by

$$\frac{x_2-x_1}{x_1}=\frac{\sin2(\theta+\Delta\theta)}{\sin2\theta\{1+(\cos2\theta/\cos\theta)[\sin\Delta\theta/\sin(\theta+\Delta\theta)]\}} \tag{4}$$

(see Appendix II).

Figure 3 shows how $\Delta x/x$ varies with θ for $\Delta\theta=2\frac{1}{2}$ and 5°. One finds that at $\theta=30°$, $\Delta x/x$ is very small. One can also

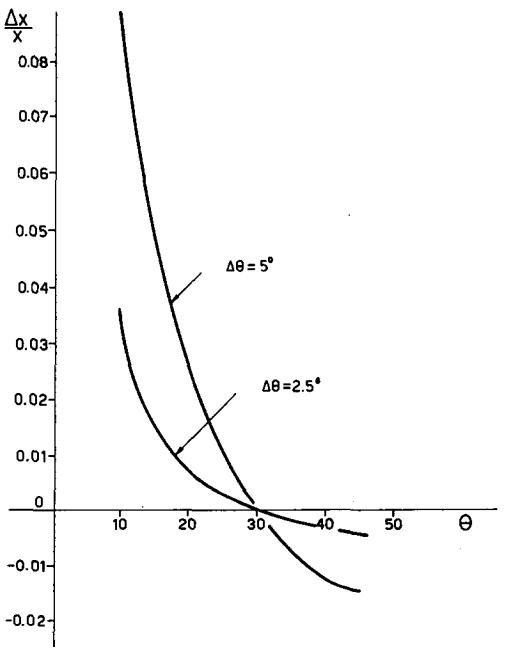

FIG. 3. Variation of angular aberration (measured as $\Delta x/x$) with mean angle θ for entrance angular apertures $\Delta\theta$ of $2\frac{1}{2}$ and 5°.

plot $\Delta x/x$ vs $\Delta\theta$ for each choice of θ; in Fig. 4 we give the calculated values for $\theta=30$ and $=45°$, the latter being used in the previous analyzers.[4,5]

The lower angular aberration at 30° can be demonstrated using a Taylor expansion for Δx in terms of $\Delta\theta$

$$\Delta x=\Delta\theta\frac{dx}{d\theta}+\frac{(\Delta\theta)^2}{2}\frac{d^2x}{d\theta^2}+\frac{(\Delta\theta)^3}{6}\cdot\left(\frac{d^3x}{d\theta^3}\right)$$

$$=\frac{2V}{E}\left[\cdot\frac{2(\Delta\theta)^2\cos3\theta}{\sin\theta}-\frac{2}{3}\left(\frac{3\sin3\theta\sin\theta+\cos3\theta\cos\theta}{\sin^2\theta}\right)(\Delta\theta)^3\right]$$

$$+\text{higher order terms.} \quad (5)$$

For $\theta=30°$

$\Delta x=-(8V/E)\cdot(\Delta\theta)^3$ (one has second order focusing), while for $\theta=45°$

$$\Delta x=\frac{4V}{E}\cdot(\Delta\theta)^2-\frac{8}{3}\cdot\frac{V}{E}\cdot(\Delta\theta)^3.$$

We have given above the calculation of the aberrations on the focal plane, showing that quadratic terms can be made zero. Calculations have also shown that the line of least confusion lies not on this plane, but at a plane slightly inclined to it which varies with the angular range being accepted—for which reason we have studied only the focal plane properties. This is an example of the case treated in light optics where it has been shown that if aberrations in the image plane can be reduced to third order then the circle of least confusion lies in another plane.[6] We are indebted to the referee for pointing out this analogy.

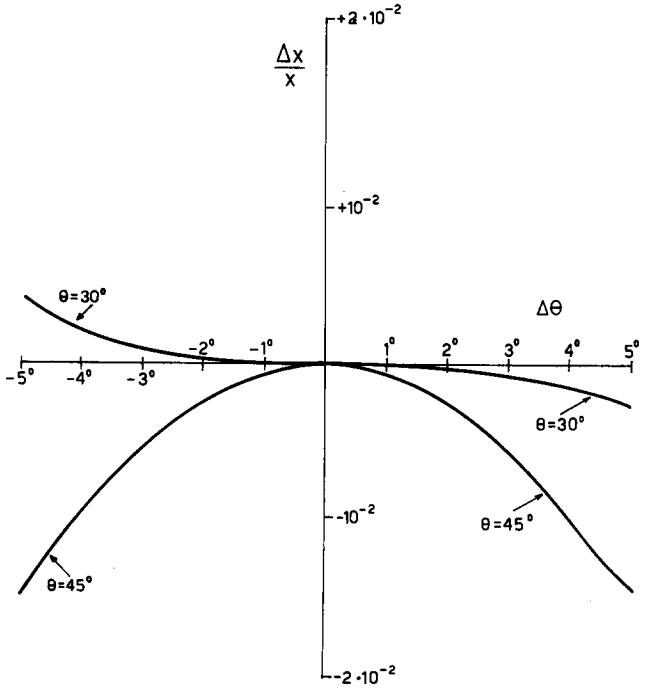

FIG. 4. Variation of angular aberration (measured as $\Delta x/x$) with angular aperture $\Delta\theta$, at mean entrance angles of 30 and 45°.

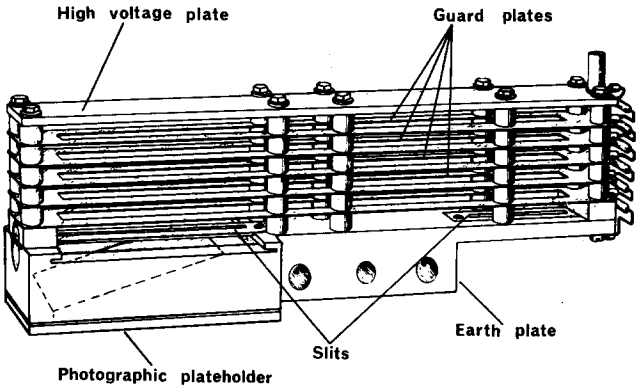

FIG. 5. Photograph of prototype analyzer being tested.

D. Magnification

It might be thought that an instrument of this nature would have magnification of unity, but due to the steep inclination of the issuing rays relative to the focal plane this may not be true. Again the procedure for calculation is straightforward; one takes a ray issuing from a point other than $(0, h)$. Suppose the source is parallel to the x axis. Then the point would be $(\pm\omega, h)$ and one calculates the difference in the intercept of the mean ray and the displaced ray. The result is (see Appendix III)

$$\Delta x/x=\omega(1+\cos2\theta),$$

which corresponds to a magnification M,

$$M=(1+\cos2\theta), \quad (6)$$

which is unity for θ equal to 45°, but 1.5 for θ equal to 30°.

E. Motion in Transverse Plane

The electric field does not, to first order, affect the motion of particles in the z plane. (In a practical model with slits and guard plates there will be fringing fields with components along the z direction.) Hence a particle emitted from the source $(0,h)$ at an angle β to the $0xy$ plane with velocity v_0 will have a velocity $v_0\cos\beta$ in that plane and a velocity $v_0\sin\beta$ along the z axis. The focusing properties are not altered, but the intercept on the focal plane decreases as one alters β; one obtains a curved image

$$\Delta x=\beta^2x_0$$

$$z=\beta x_0.$$

If particles are emitted from a point not on the $0xy$ plane, the image is displaced. Clearly if the source has a width $\pm z_0$ on the z axis, the resultant image projection on the x axis is given by

$$\Delta x=z^2_0/x_0,$$

or

$$\Delta x/x=(z_0/x)^2.$$

This image size results if the transverse angular acceptance

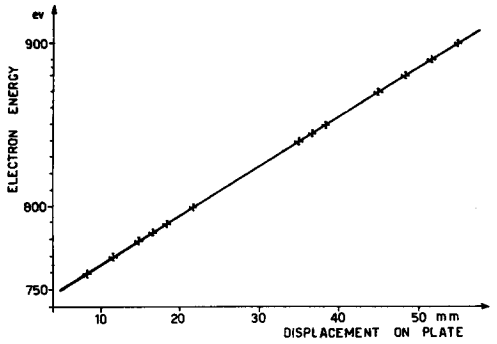

FIG. 6. Relationship between energy and position on focal plane. Curve is theoretical, points experimental.

is sufficiently large. Increase of the acceptance above the value $\beta=z_0/x_0$ does not change the resolution attainable, it increases the transverse image size.

F. Energy Range of the Instrument

In the specific case of θ equal to 30°, the equation of the focal line [Eq. (3)] becomes

$$x=3\sqrt{3}(h+y).$$

The minimum recorded energy is for y equal to zero and the corresponding focus is at

$$x=3\sqrt{3}h.$$

The parameter h will generally be fixed by the details of the experimental environment for the spectrograph. The maximum energy will correspond to a focus at $x_{\max}$ which is the maximum physical dimension allowable for the spectrograph. The range of energies R observable is therefore given by

$$R=V_{\max}/V_{\min}=x_{\max}/3\sqrt{3}h. \quad (7)$$

II. DESIGN AND TESTING OF AN INSTRUMENT

Many factors can influence the choice of design parameters h, E and energy range for a given instrument. In the design considered in our institute the main restrictions were on h, which is essentially the spacing of the source, and the total size. This fixed the fractional energy range which could be investigated [Eq. (7)]. The maximum energy was chosen to be 1 keV.

The following parameters were used: $h=4$ cm, $x_{\max}=30$ cm, d (electrode spacing) $=5$ cm, $E=80$ V/cm. The electrode spacing of 5 cm was chosen to allow the trajectories of the extreme rays of 36° to pass through the instrument.

The entrance window to the analyzer (see Fig. 5) was a slit 50 mm long and 3 mm wide, without a grid. As commented below it was found that field distortion in the slit gave rise to modification of the curve of angular aberrations. The exit slit was 90 mm long and 3 mm wide. Measurements were made with electrons which were recorded on a photographic plate. Guard electrodes were mounted at each 0.8 cm, their potentials being subdivisions of the total to an accuracy of 1%. Each guard electrode extended for 1 cm beyond the volume being used.

Tests were carried out of dispersion, angular aberrations, and resolution, using a 900 eV electron beam. It was necessary to keep the beam current below a value of 10^{-8} A, in order that space charge expansion of the beam should not cause a deterioration of the resolution.[7,8] The energy dispersion on the photographic plate was found to be constant along the plate and had a value of 0.33 mm/V (see Fig. 6) compared with the theoretical value of 0.331 mm/V. At one energy, a narrow beam ($s=1$ mm, $\Delta\theta=1°$) was swept in θ from 24 to 36° to test the theoretical predictions. Results are shown in Fig. 7.

Some difficulty was encountered in obtaining the required accuracy of positioning while changing angle, and this could account for the scatter of observations. The definite trend at low angles for the aberration to be lower than predicted was found to be due to deformations of the electric field at the extreme low angle end of the entrance slit. These deformations have been measured in a resistive paper model: Experimentally we have varied the slit length and found that agreement with theory is better the longer is the slit (see Fig. 7).

Finally, Fig. 8 shows data taken with a wide beam (±6°), and a transverse angular spread of 2° for a source slit of 1 mm with different beam energies. It can be seen that the resolution is in fact better than 0.5%.

III. COMPARISON WITH OTHER ANALYZERS

Throughout the text we have made comparisons with the 45° entrance angle analyzer, showing that a 30° entrance angle yields better resolution. Writing the spread $\Delta x/x$ as $\Delta E/E$ we have

$$30° \text{ analyzer} \quad \Delta E/E\simeq 1.6(\Delta\theta)^3$$
$$45° \text{ analyzer} \quad \Delta E/E\simeq 1.4(\Delta\theta)^2.$$

Both instruments are of course broad range spectrographs.

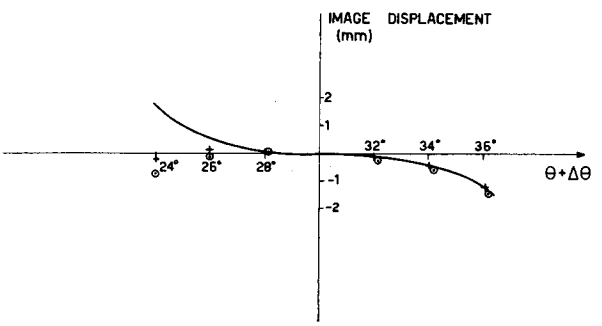

FIG. 7. Experimental data on angular aberrations compared with theoretical predictions. Data marked + are for entrance slit 4.6 cm long; those marked ⊙ are for slit 5.2 cm long.

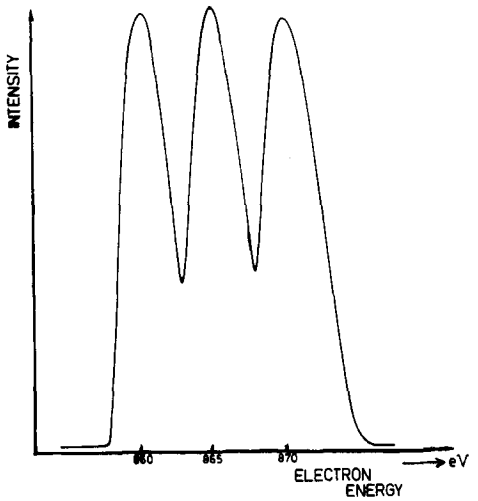

FIG. 8. Spectra obtained with electron beam with angular spread ±6°.

A number of analyzers exist which are designed to give high energy resolution for wide angular acceptance but are essentially monochromators. It is instructive to compare resolution factors.

(a) 127° analyzer. In this case $\Delta E/E=\frac{4}{3}(\Delta\theta)^2$.

(b) Spherical analyzer. The spherical analyzer,[3] which has the property of providing two dimensional focusing, gives only first order focusing and one has

$$\Delta E/E=(\Delta\theta)^2.$$

(c) Cylindrical mirror. Another analyzer which yields two dimensional focusing is the cylindrical mirror.[9,10] With a special choice of entrance angles second order focusing can be achieved yielding a value of $\Delta E/E\simeq 2.8(\Delta\theta)^3$. One should note, of course, in this case as in the analyzer we describe in the text a source of divergence $\pm\Delta\theta$ will give an energy width double the values given above, while in the analyzers with only first order focusing and corresponding quadratic aberrations, this is not the case.

ACKNOWLEDGMENTS

The authors wish to express their gratitude to F. Renaud and M. Galanti for their assistance in the mechanical design and testing of the analyzer.

APPENDIX I: CALCULATION OF PARTICLE PATH

From S to A (Fig. 2) the particle travels in a straight line intercepting the x axis at

$$x=h\cot\theta.$$

Inside the analyzer region,

$$\ddot{y}=Ee/m$$
$$\ddot{x}=0.$$

Hence $$y=Eet^2/2m+\dot{y}_0t,$$

where $\dot{y}_0$ is value at entrance to field equals $-v\sin\theta$. The particle returns to the plate ($y=0$) after a time t, where

$$t=2mv\sin\theta/Ee.$$

The displacement along the x axis in this time is $\dot{x}t$, i.e.,

$$2mv^2\sin\theta\cos\theta/Ee.$$

Finally after exit the particle travels in a straight line at an angle θ to the x axis, and the further x displacement is

$$x=y\cot\theta.$$

Total displacement

$$x=(h+y)\cot\theta+(2V/E)\sin2\theta,$$

where V is the kinetic energy in electron volts.

APPENDIX II: ANGULAR ABERRATION

Figure 9 shows the paths of two rays leaving the source with different angles, θ and $\Delta\theta$. We wish to calculate the displacement of ray 2 from ray 1 along the focal line.

For ray 1

$$x=(h+y)\cot\theta+(2V/E)\sin2\theta.$$

For ray 2

$$x=(h+y)\cot(\theta+\Delta\theta)+(2V/E)\sin2(\theta+\Delta\theta).$$

Focal line is

$$x=(h+y)\cot\theta\cdot[1+(1/\cos2\theta)].$$

Hence x, the intercept of ray 1 with the focal line is given by

$$x_1=(2V/E)\sin2\theta(1+\cos2\theta)$$

and x_2, the intercept of ray 2 with the focal line, by

$$x_2=\frac{2V}{E}\frac{\sin2(\theta+\Delta\theta)}{\{1-[\tan\theta/\tan(\theta+\Delta\theta)][\cos2\theta/(1+\cos2\theta)]\}}.$$

The x displacement of the intercepts is then

$$\Delta x=x_2-x_1$$

and

$$\frac{\Delta x}{x_1}=\frac{\sin2(\theta+\Delta\theta)}{\sin2\theta[1+(\cos2\theta/\cos\theta)\cdot[\sin\Delta\theta/\sin(\theta+\Delta\theta)]\}}.$$

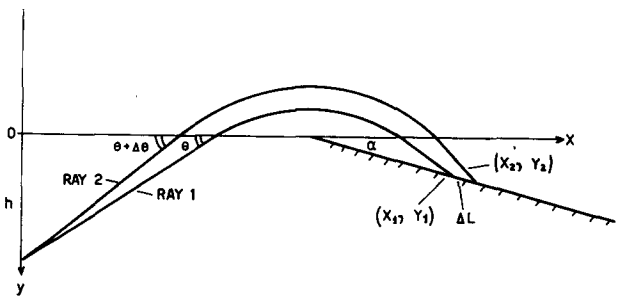

FIG. 9. Ray paths used to calculate angular aberration.

APPENDIX III: CALCULATION OF MAGNIFICATION AND OF PRECISION OF CONSTRUCTION

In the analysis given above we have calculated the position of the focal line and the intercepts x_1, x_2 of two rays with this line when the rays have angles θ, $\theta+\Delta\theta$, and originate from the point $(0,h)$. We now consider the more general case in which the source is at (s,h_1) and has a width 2ω, so that we take extreme rays, one from (s,h_1) with angle θ, the other from $(s+\omega,h_1)$ with angle $\theta+\Delta\theta$. We take the focal plane to be correctly positioned for a source $(0,h_0)$ angle θ.

For ray 1

$$x=(h_1+y)\cot\theta+(2V/E)\sin2\theta+s.$$

For ray 2

$$x=(h_1+y)\cot(\theta+\Delta\theta)+(2V/E)\sin2(\theta+\Delta\theta)+s+\omega.$$

Focal line is

$$x=(h_0+y)\cot\theta(1+1/\cos2\theta).$$

Hence the intercept x_1 is given by

$$x_1=(h_1-h_0)\cot\theta(1+\cos2\theta)+\frac{2V}{E}\sin2\theta(1+\cos2\theta)+s(1+\cos2\theta),$$

and

$$x_2\left[1-\frac{\cot(\theta+\Delta\theta)}{\cot\theta}\cdot\frac{\cos2\theta}{1+\cos2\theta}\right]=\frac{2V}{E}\sin2(\theta+\Delta\theta)+s+\omega+(h_1-h_0)\cot(\theta+\Delta\theta).$$

We can take the difference in intercepts x_2-x_1 and write

$$x_2-x_1=\frac{2V}{E}\sin2\theta(1+\cos2\theta)\left\{\frac{\sin2(\theta+\Delta\theta)}{\sin2\theta\{(1+\cos2\theta)-[\tan\theta/\tan(\theta+\Delta\theta)]\cos2\theta\}}-1\right\}$$
$$+s(1+\cos2\theta)\left\{\frac{1}{(1+\cos2\theta)-[\tan\theta/\tan(\theta+\Delta\theta)]\cos2\theta}-1\right\}+\omega(1+\cos2\theta)\left\{\frac{1}{(1+\cos2\theta)-[\tan\theta/\tan(\theta+\Delta\theta)]\cos2\theta}\right\}$$
$$+(h_1-h_0)(1+\cos2\theta)^2[\cot(\theta+\Delta\theta)-\cot\theta]\cdot\left\{\frac{1}{1+\cos2\theta-[\tan\theta/\tan(\theta+\Delta\theta)\cos2\theta]}\right\}.$$

The terms occurring in this equation can be identified with the following errors:

First term: angular aberrations as given in Appendix II.

Second term: is s error in positioning of the source along the x axis, $x_2-x_1\simeq s\Delta\theta$. Since $\Delta\theta\simeq\pm0.1$ rad we require $s<1$ mm to produce negligible effect.

Third term: is the magnification and depends very slightly on $\Delta\theta$, $x_2-x_1\simeq\omega(1+\cos2\theta)$. Hence the magnification is $(1+\cos2\theta)=1.5$.

Fourth term: is the error term in h and is given for $\theta=30°$ by

$$x_2-x_1=9(h_1-h_0)\cdot\Delta\theta.$$

Consequently one must locate the source on the y axis to an accuracy of 0.11 mm to give $x_2-x_2=0.1$ mm for $\Delta\theta=0.1$ rad. It is clear that this expression also gives the error which arises from correct positioning of the source but wrong positioning of the focal plate.

[1] H. S. Bridge, C. Dilworth, B. Rossi, F. Scherb, and E. F. Lyon, J. Geophys. Res. **65**, 3053 (1960).
[2] A. L. Hughes and V. Rojansky, Phys. Rev. **34**, 284 (1929).
[3] E. M. Purcell, Phys. Rev. **54**, 818 (1938).
[4] G. A. Harrower, Rev. Sci. Instrum. **26**, 850 (1955).
[5] G. D. Yarnold and H. C. Bolton, Rev. Sci. Instrum. **26**, 38 (1964).
[6] A. E. Conrady, *Applied Optics and Optical Design* (Dover, New York, 1957), pp. 120 ff.
[7] H. H. Fleishmann, D.E.T.F. Ashley, and A. V. Larson, Nucl. Fusion **5**, 349 (1965).
[8] R. François and M. Barat, Compt. Rend. **266**, 1306 (1968).
[9] V. V. Zashkavara, M. I. Korsunskii, and O. S. Kosmachev, Sov. Phys. JETP **11**, 96 (1960).
[10] H. Z. Zar-el, Rev. Sci. Instrum. **38**, 1210 (1967).